AD A139581

Seismo-Acoustic Effects of Sonic Booms on Archeological Sites, Valentine Military Operations Area

JAMES C. BATTIS

9 November 1983

DTIC
ELECTE
APR 2 1984
S
A

TERRESTRIAL SCIENCES DIVISION   PROJECT 7600
AIR FORCE GEOPHYSICS LABORATORY
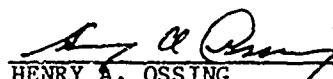HANSCOM AFB, MASSACHUSETTS 01731

AIR FORCE SYSTEMS COMMAND, USAF

84 03 27 035

This report has been reviewed by the ESD Public Affairs Office (PA) and is releasable to the National Technical Information Service (NTIS).

This technical report has been reviewed and is approved for publication.

FOR THE COMMANDER

HENRY A. OSSING
Chief, Solid Earth Geophysics Branch
Earth Sciences Division

DONALD H. ECKHARDT
Director
Earth Sciences Division

Qualified requestors may obtain additional copies from the Defense Techical Information Center. All others should apply to the National Technical Information Service.

If your address has changed, or if you wish to be removed from the mailing list, or if the addressee is no longer employed by your organization, please notify AFGL/DAA, Hanscom AFB, MA 01731. This will assist us in maintaining a current mailing list.

Do not return copies of this report unless contractual obligations or notices on a specific document requires that it be returned.

ADA139 581

REPORT DOCUMENTATION PAGE

1a. REPORT SECURITY CLASSIFICATION	1b. RESTRICTIVE MARKINGS		
Unclassified			
2a. SECURITY CLASSIFICATION AUTHORITY	3. DISTRIBUTION/AVAILABILITY CF REPORT		
2b. DECLASSIFICATION/DOWNGRADING SCHEDULE	Approved for public release; distribution unlimited.		
4. PERFORMING ORGANIZATION REPORT NUMBER(S)	5. MONITORING ORGANIZATION REPORT NUMBER(S)		
AFGL-TR-83-0304 ERP, No. 858			

6a. NAME OF PERFORMING ORGANIZATION	6b. OFFICE SYMBOL (If applicable)	7a. NAME OF MONITORING ORGANIZATION
Air Force Geophysics Laboratory	LWH	
6c. ADDRESS (City, State and ZIP Code)		7b. ADDRESS (City, State and ZIP Code)
Hanscom AFB, Massachusetts 01731		

8a. NAME OF FUNDING/SPONSORING ORGANIZATION	8b. OFFICE SYMBOL (If applicable)	9. PROCUREMENT INSTRUMENT IDENTIFICATION NUMBER		
Air Force Geophysics Laboratory	LWH			
8c. ADDRESS (City, State and ZIP Code)		10 SOURCE OF FUNDING NOS.		
Hanscom AFB, Massachusetts 01731		PROGRAM ELEMENT NO.	PROJECT NO.	TASK NO. / WORK UNIT NO.

10 SOURCE OF FUNDING NOS.			
PROGRAM ELEMENT NO.	PROJECT NO.	TASK NO.	WORK UNIT NO.
62101F	7600	09	05

11. TITLE (Include Security Classification)
See Reverse Side

12. PERSONAL AUTHOR(S)
James C. Battis

13a. TYPE OF REPORT	13b. TIME COVERED	14 DATE OF REPORT (Yr., Mo., Day)	15. PAGE COUNT
Scientific. Interim.	FROM _____ TO _____	1983 October 11	36

16. SUPPLEMENTARY NOTATION

17. COSATI CODES			18. SUBJECT TERMS (Continue on reverse if necessary and identify by block number)
FIELD	GROUP	SUB GR.	Seismic motions Seismo-acoustic effects
			Sonic booms

19. ABSTRACT (Continue on reverse if necessary and identify by block number)
Seismo-acoustic recordings of sonic booms were made at two sites in the Valentine Military Operations Area (MOA). Each location was selected as representative of a class of significant archeological sites found within the MOA. These studies indicate that sonic booms are unlikely to cause damage to the archeological finds. The expected motions are, at worst, 8 percent of the limits set by strict blasting codes and comparable to velocities that could be produced by local earthquakes which have occurred in the Valentine area. At these levels of motion, competent rock will be unaffected by the transmission of seismic waves. The predicted velocity levels are unlikely to initiate either fracture or spalling in rocks. However, it is possible that in rocks where natural meteorological action has initiated these erosive mechanisms the sonic boom induced motion could accelerate the processes to some small, and probably insignificant, degree.

20. DISTRIBUTION/AVAILABILITY OF ABSTRACT	21. ABSTRACT SECURITY CLASSIFICATION
UNCLASSIFIED/UNLIMITED ☒ SAME AS RPT. ☒ DTIC USERS ☐	UNCLASSIFIED
22a. NAME OF RESPONSIBLE INDIVIDUAL	22b TELEPHONE NUMBER (Include Area Code) / 22c. OFFICE SYMBOL
James C. Battis	(617)861-3222 LWH

DD FORM 1473, 83 APR   EDITION OF 1 JAN 73 IS OBSOLETE.

Contents

Illustrations

Table

6

Seismo-Acoustic Effects of
Sonic Booms on Archeological Sites,
Valentine Military Operations Area

1. INTRODUCTION

During the period 16 to 18 July 1981, AFGL/LWH participated in a field pro-
gram designed to study the effects of sonic booms on significant archeological
sites located within the Valentine, Texas, Military Operations Area (MOA). This
effort was in response to a request from The Environmental Planning Division at
Headquarter·., Tactical Air Command (HQ TAC/DEEV) to assist in the environ-
mental impact assessment being conducted as part of the process required to
redesignate the Valentine MOA from subsonic to supersonic operations. In addi-
tion to personnel from LWH and DEEV, the Texas State Historical Preservation
Office and the Texas Bureau of Economic Geology participated in the field program.

This investigation was primarily directed at determining the potential for
damage by sonic booms to American Indian rock shelter and petroglyph sites
located within the MOA. The rock shelters consist of caves located in hard rock
formations such as cliffs that form canyon walls and mountain slopes. Pictographs
are often found on the rock surfaces of these caves. Petroglyphs can be found on
any hard rock surface including rock outcrops and free standing boulders. While
other possible archeological sites were not explicitly considered, the data pro-
vided ¹n this paper cover a wide range of the geologic settings found in the

Valentine MOA and can be used for estimation of seismo-acoustic effects of sonic booms at other possible sites.

During this study, seismic and acoustic sensors were used to record the effects of sonic booms at locations similar to the significant archeologic sites within the Valentine MOA. Based on these records, estimates are made of peak ground velocities at the archeological sites that could result from supersonic operations over the Valentine MOA. These levels of motion are compared to other, more common, sources of seismic motions. In addition, a similar sonic boom test was performed in Railroad Valley, Nevada, and the results of this test are applied to determine the implications for damage to historic artifacts within the Valentine MOA.

2. SEISMO-ACOUSTIC EFFECTS OF SONIC BOOMS

Under most conditions, it can be assumed that the ground surface responds as a rigid body to acoustic waves propagating through the atmosphere. The incident pressure wave is reflected off the surface without energy loss. This is a consequence of the large density contrast between air and ground. The incident and reflected pressures are of equal amplitude.

In reality, the atmosphere and ground are not completely decoupled and low level ground motions are induced by acoustic waves. The amplitude of the induced motion will be larger in soils than in hard rock. Under certain limited conditions the induced ground motion can become much larger than usual. These amplified seismic waves, known as air-coupled surface waves, can be generated when the shallow ground structure consists of a thin, low velocity layer over a layer of much higher velocity.[1] If the velocity of the surface layer approaches the speed of sound in air, the seismic wave travels with the acoustic wave and the amplitude of the seismic motion is reinforced or amplified. Alluvial basins, such as found in the Valentine MOA, typically have velocity structures that support air-coupled surface waves.

3. FIELD STUDIES

Acoustic and seismic measurements of sonic booms and the induced ground motions were conducted at two locations in the Valentine MOA. These sites were chosen for topographic and geologic similarity to significant archeological sites

---

1. Haskell, N. (1951) A note on air-coupled surface waves, Bull. Seism. Soc. Amer. 41:295-300.

identified by the Texas State Historical Preservation Office. The actual test locations were suggested by a geologist from the Texas Bureau of Economic Geology and accepted with the concurrence of the other participating offices. A brief description of each site is given in the following sections.

3.1 Rock Shelter Site

The first site occupied was located in the Van Horn Mountains at approximately $30°48.7N$ and $104°51.4W$. The general area contained at le. caves or rock shelters of natural origin in competent rhyolitic rock. The caves were located in a north to northwest facing cliff at an elevation of 1525 m MSL (5000 ft MSL). The caves at this site showed evidence of human habitation including pictographs.

The geologic setting of this site precluded the generation of significant air-coupled seismic waves as would be expected in a site located on the floor of an alluvial basin. However, topographic amplification of the acoustic or seismic waves inside the rock shelters as compared to outside the caves was considered a possible effect. To examine this problem, acoustic pressure transducers and vertical seismometers were deployed at two locations. One system was installed on a cave floor and the other on a rock outcrop about 50 m (160 ft) from the instrumented cave. The second location was considered to be free of any topographic effects and thus representative of the free-field acoustic and seismic motions. As the pictographs were drawn on the rock walls of the shelters, both seismometers were placed on hard rock. The use of only vertical seismometers is justified by the fact that vertical ground motion is generally the largest of the three components of motion produced by sonic booms.

3.2 Boulder Field Site

The second site examined in this effort was selected for its similarity to the geology of the Lobos Canyon petroglyph site. The test locale consisted of boulders and outcrops of Cox sandstone situated on an alluvial fan at the western base of the Van Horn Mountains. This site was at an elevation of approximately 1300 m MSL (4300 ft). The coordinates of the site were $30°50'N$ and $104°54'W$.

At this site the primary concern was the efficiency of coupling between ground motion induced in the soil of the alluvial fan and the rock outcrops and boulders. Instrumentation at this location included one pressure transducer, a vertical seismometer and a horizontal seismometer with its axis oriented along the north-south direction. These instruments were placed on an outcrop in the boulder field.

Although most Lobos Canyon petroglyphs are pecked on boulders, petroglyphs located on rock outcrops are threatened more than those on boulders by the

seismo-acoustic effects of sonic booms. Motion in boulders and outcrops of rock on the alluvial fan can be generated in two ways. First, the acoustic wave hitting the boulder or outcrop surface directly will develop motions within the rock. The amplitude of this motion is not expected to be appreciably different in boulders and outcrops. Second, ground motions generated in the alluvium can be trans-mitted to the boulder or outcrop. A boulder whose base is slightly buried in the alluvium will respond as a rigid body to motions of the frequencies expected in this problem. In other words, the boulder will respond like a cork floating on ocean waves. With no vibrations occurring internally to the boulder the potential for damage is extremely small. For outcrops, however, the seismic motion can be transmitted into the rock and thus a higher damage potential exists. The response of a large outcrop to the seismo-acoustic motions produced by sonic booms should represent the upper limit of boulder response.

3.3 Supersonic Overflights

Ten supersonic flights were made over the two locations just described. Six flights occurred while the rock shelter site was occupied and four flights were conducted over the boulder field site. All passes were made by F-15 aircraft flying at Mach 1.1 and at altitudes of 4570 and 6100 m MSL (15,000 and 20,000 ft). For an F-15 aircraft flying at the specified altitudes and speed, the peak over-pressures expected to be observed ranged from 139.3 to 203.0 Pa (2.9 to 4.2 psf).[2]

Of the ten sonic booms generated, only two were audibly or instrumentally detected at the ground level. It is assumed that the sonic booms generated in the remaining eight overflights were dissipated in the atmosphere without reaching the ground. This could result from atmospheric conditions such as a strong temperature gradient between the aircraft operating altitudes and ground level.

4. DATA ANALYSIS

4.1 Rock Shelter Site

In Figure 1, the seismic and acoustic records of the one sonic boom observed at the rock shelter site are shown. Pressure transducers in both the free-field and the cave recorded an acoustic N-wave (see Section 5.1) having a duration of 0.32 sec and peak over-pressure of 4.9 Pa (0.10 psf). The sonic boom was produced on an east to west pass over the site with the aircraft at 6100 m MSL (20,000 ft). This flight path is in line with the cave opening.

2. (1979) Draft Environmental Impact Statement, Supersonic Flight Operations in the Valentine Military Operations Area, Dept. of the Air Force, Holloman AFB, New Mexico.
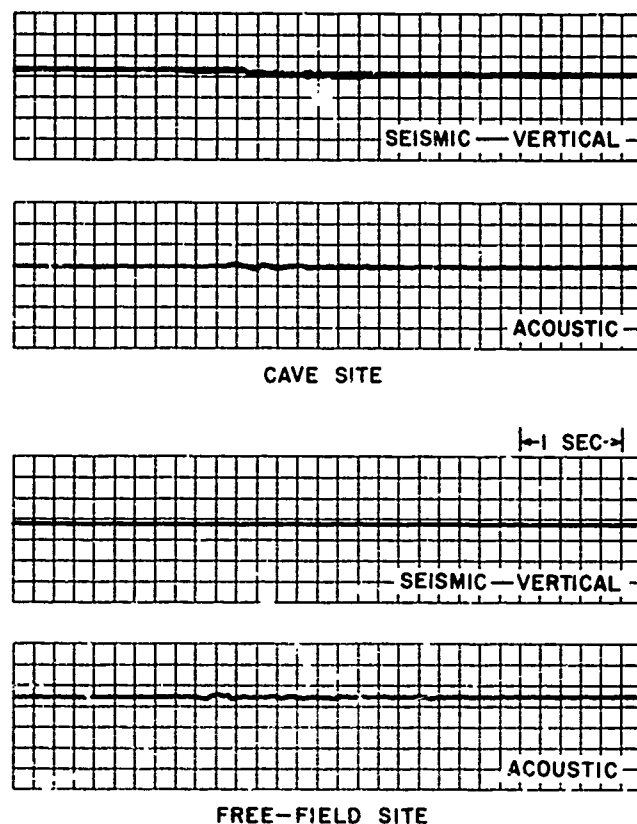
Figure 1. Seismic and Acoustic Records of
a Sonic Boom Recorded at the Rock Shelter
Site

As the expected over-pressures were much higher than those actually observed, the seismograph gains were set relatively low. This resulted in no detectable ground motion at the free-field site and barely discernible motion on the cave instrument. The low amplitude motions at the cave prevent the accurate evaluation of the frequency of this signal, although a lower limit of 25 Hz can be estimated. Using a conservative estimate of 50 Hz, the acoustically induced ground velocity is $4.5 \, \mu m/sec$ (1.8×10^{-4} in./sec). If the frequency is 25 Hz then the velocity is $2.5 \, \mu m/sec$ (9.7×10^{-5} in./sec). The variation in amplitude results from the frequency dependence of the instrument response. The signal arrives in several packets over a time window of 0.48 sec.

The lack of detectable seismic motion at the free-field site is not unexpected. The velocity recorded at the cave is very close to the detection threshold of the

11

instrument system as deployed. If either the instrument response were lower or the instrument-ground coupling were poorer at the free-field site than at the cave site, no motion would be recorded even though the actual ground motions at each site were identical. In fact, the free-field site appeared to have poorer coupling between the ground and the seismometer than the cave site.

4.2 Boulder Field Site

The N-wave recorded at the boulder field site was very similar to that recorded at the rock shelter. A peak over-pressure of 5.9 Pa (0.12 psf) with N-wave duration of 0.32 sec was recorded. The acoustic and seismic traces of this event are shown in Figure 2. This sonic boom was also recorded from an east to west overpass at an altitude of 6100 m MSL (20 000 ft).
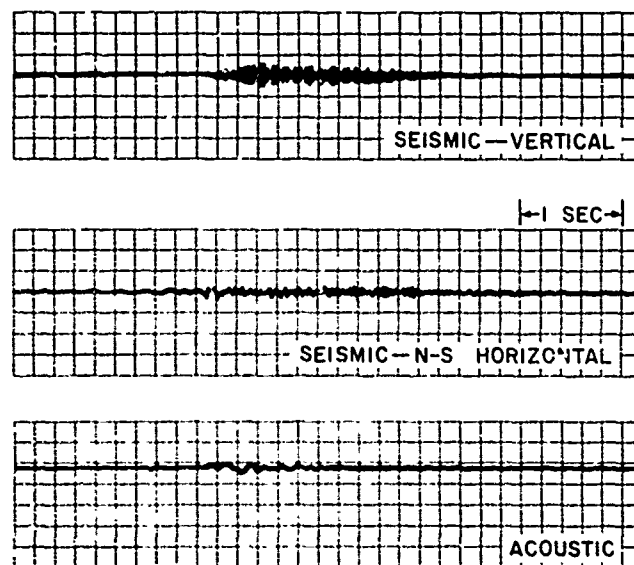
Figure 2. Seismic and Acoustic Records of a Sonic Boom Recorded at the Boulder Field Site

The peak velocity of the North-South oriented horizontal seismometer was found to be 5.7 μm/sec (2.2 X 10^{-4} in./sec), at a frequency of 30 Hz.

It should be noted that due to instrument response effects, this motion is not the maximum trace displacement, but occurs in one of the late arriving packets of energy. The peak vertical velocity occurs approximately 0.5 sec into the record

12

and has an amplitude of 7.5 μm/sec (2.9 × 10^{-4} in./sec). The frequency of the vertical motion is 30 Hz and is uniform throughout most of the record. Vertical signal duration is 3.48 sec.

The primary phase on the vertical seismometer is an air-coupled acoustic wave with an interference pattern typical of multipathing. Physical constraints require that the air-coupled surface wave was generated in the alluvial material and not in the rock outcrop. Its appearance on a record made at a hard rock site indicates coupling between the alluvial material and the outcrop. The 30-Hz frequency is higher than normally expected for the dominant frequency of the air-coupled wave. Values in the range of 10 to 20 Hz are more common in alluvial basins. (Henry Ossing, personal communication.) The higher frequency can be explained in either of two ways. First, the geologic layering in the alluvial fan cannot support the lower frequencies. Second, the lower frequency waves were generated in the alluvium but were not efficiently transmitted to the rock outcrop. Given the available data, one explanation cannot be shown to be superior to the other.

As stated above, the vertical record exhibits an interference pattern characteristic of multipathing. Multipathing is the condition where almost identical seismic signals arrive at the seismometer along two or more different paths with a small time delay between arrivals. The cause of this multipathing is likely to be local geologic irregularities. This phenomenon causes amplitude modulation of the signal with time and with the effect of increasing the reported peak velocity as compared to a signal transmitted along a single path.

4.3 Acoustic Admittances

Acoustic admittance is defined as the ratio of peak velocity to peak over-pressure at specified frequencies. If $Y(f)$ is the admittance, $V_{max}(f)$ is the peak velocity, and $P_{max}(f)$, the maximum over-pressure at a specified frequency, then:

$$Y(f) = V_{max}(f)/P_{max}(f) \tag{1}$$

Under linear elastic assumptions, the admittance at any frequency is a fixed ratio of induced ground motion to input over-pressure. Strictly, it is also a function of the angle at which the sonic boom hits the ground. For sonic booms in the range 23.5 to 239.3 Pa (0.5 to 5.0 psf) the linear response of ground motion to over-pressure has been empirically demonstrated.[3] Acoustic admittance is typically calculated as the spectral ratio of the seismic and acoustic signals.

---

3. Goforth, T., and McDonald, J. (1968) Seismic Effects of Sonic Booms, NASA Report No. CR-1137, Teledyne Geotech, Garland, Tex.

Due to the limitations of the available data a modified admittance value is calculated for the two sites investigated. In this case, the absolute peak over-pressure is used in place of $P_{max}(f)$. As the relative spectral characteristics of the N-wave are uniform for a given aircraft, this modification is not significant as long as the use of this value is restricted to the specific aircraft or one producing a similar N-wave spectrum.

For the rock shelter site the calculated admittance is 0.91 (μm/sec)/Pa $[1.7 \times 10^{-3}$ (in./sec)/psf] at 50 Hz. A value of 1.27 (μm/sec)/Pa $[2.4 \times 10^{-3}$ (in./sec)/psf] at 30 Hz was found at the boulder site. These values are comparable to an admittance of 1.57 (μm/sec)/Pa $[3.0 \times 10^{-3}$ (in./sec)/psf] found as a typical value for hard rock.[3]

5. EMPIRICAL EVALUATION

5.1 Acoustic Effects

The peak over-pressure for carpet booms generated during supersonic operations over the Valentine MOA is estimated to be 248.1 Pa (5.2 psf).[2] For a sonic boom this pressure is applied impulsively to the ground. To fracture most rocks much higher levels of pressure must be applied continuously to failure. Laboratory measurements of the crushing strengths of rocks at low confining pressures and normal temperatures show a wide variability depending on the actual rock type and condition.[4] A value of 9.8×10^5 Pa $(2.1 \times 10^4$ psf) is a conservative lower limit. More typical values are between 10 and 200 times this pressure. In any case, this lower limit is 4000 times the over-pressure generated by a sonic boom. Tensile strengths are typically lower than compressive strengths by a factor of 5 to 15.[5] These values are still 260 times the sonic boom over-pressures expected over the Valentine MOA. In addition, rock, as with most other material, can withstand higher stresses applied impulsively rather than continuously.

5.2 Blasting Codes

Strict blasting codes typically limit the peak vector sum ground velocity to less than 2.6×10^4 μm/sec (1.0 in./sec) at the structure closest to the blasting point and not owned by the company doing the blasting.[6] The vector sum velocity

4. Handin, J. (1966) Strength and Ductility, in Handbook of Physical Constants, S. Clark, Jr., Ed., The Geol. Soc. Amer., New York, N.Y.

5. Jaeger, J.C., and Cook, N.G.W. (1969) Fundamentals of Rock Mechanics, Methuen & Co. Ltd, London.

6. Dade County, Florida Code, Section 13-12.

is defined as the square root of the sum of the squares of the velocities in the three components of motion. This value is approximately one-half the ground velocity at which the potential for damage to buildings exists.[7] The complex structural response of buildings makes them more sensitive to motion than rock is likely to be.

Supersonic operations over the Valentine MOA are expected to generate carpet booms with over-pressures below 248.1 Pa (5.2 psi).[2] Using this value and the admittances calculated in Section 3.3, peak vertical ground velocities can be evaluated for the two sites studied. At the rock shelter site the maximum velocity is expected to be 225 μm/sec (8.8 $\times$ 10^{-3} in./sec) and 316 μm/sec (1.2 $\times$ 10^{-2} in./sec) at the boulder field site. Use of these vertical amplitudes as the motion levels in all three components of motion is a conservative assumption as vertical motion is generally the highest amplitude of the three components. A conservative estimate of the peak vector sum velocity at each site is then found to be 390 μm/sec (1.5 $\times$ 10^{-2} in./sec) and 547 μm/sec (2.1 $\times$ 10^{-2} in./sec), respectively. These values are less than 2.5 percent of the ground velocity limits used in blasting codes.

5.3 Earthquake Motions

The Valentine MOA includes the seismically active Marfa Basin.[8] What is believed to be the largest earthquake in Texas during historic times had an epicenter approximately 14 km (7.5 nmi) northwest of the town of Valentine. This earthquake occurred on 16 August 1931. Estimates of the magnitude of this event range between 5.6 and 5.9 m_b and 6.4 M_L. Between 1977 and 1980 numerous events with magnitudes up to 2.6 M_L were recorded instrumentally within the Valentine MOA. The epicenters of these events are also shown in Figure 3. On 1 August 1975 a poorly located earthquake of magnitude 4.8 M_L was felt in Valentine.

The location of the 16 August 1931 earthquake places it within 110 km (60 nmi) of any point within the Valentine MOA. Using a strong ground motion attentuation function of the form:

$$\ln v_s = 1.73 + 0.921 M_L - 1.20 \ln (R + 25) \tag{2}$$

7. Ortaid, L. (1972) Blasting operations in the urban environment, Assoc. Engin. Geol. 9:27-46.

8. Dumas, D., Dorman, H., and Latham, G. (1980) A reevaluation of the August 16, 1931 Texas earthquake, Bull. Seism. Soc. Amer. 70:1171-1180.
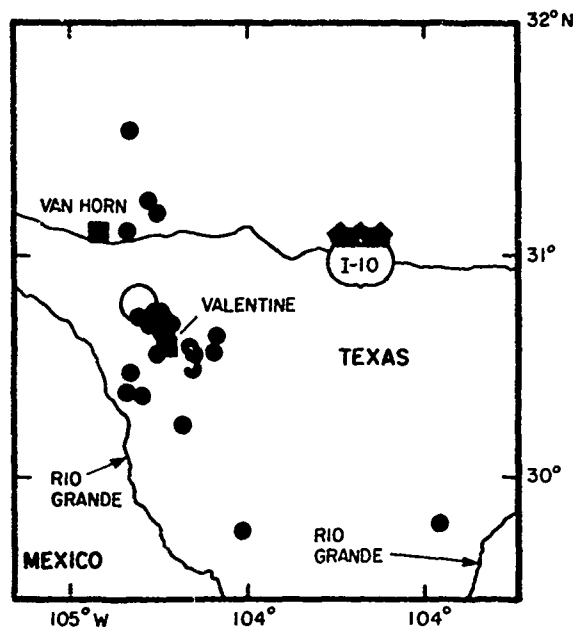
Figure 3. Earthquake Epicenters near the
Valentine MOA During the Period 1977 to 1980.
Large open circle is the epicenter of the 1931
earthquake

estimates of the peak velocities from this earthquake can be made.[9] In this
equation v_s is the site velocity in cm/sec, M_L is magnitude and R is the epicen-
tral distance in kilometers. Using a local magnitude of 5.8 M_L, equivalent to
5.6 m_b, the ground velocity from this event is found to be at least $3.3 \times 10^4 \, \mu m/$
sec (1.3 in./sec) at any location within the Valentine MOA. This value is 100
times the value estimated for sonic boom induced ground velocities. At a closer
range, 50 km, the ground motion is $6.6 \times 10^4 \, \mu m/sec$ (2.6 in./sec) or 200 times
the value of the induced motions.

The estimation of peak velocities from low magnitude, local earthquakes is a
difficult problem. However, accelerograms have been recorded at Bear Valley,
California for events of 3.0 and 3.2 M_L at distances of 2 to 10 km (1.1 to 5.4

9. McGuire, R. (1974) Seismic Structural Response Risk Analysis Incorporating
   Peak Response Regressions on Earthquakes Magnitude and Distance,
   Dept. Civil Eng. Research Report No. R47-51, Mass. Inst. Tech.,
   Cambridge, Mass.

16

nmi).[10] A peak velocity of 1.0×10^4 μm/sec (0.4 in./sec) was recorded at 2 km (1.1 nmi) for the 3.0 M_L event, 7.2×10^3 μm/sec (0.3 in./sec) at 5 km (2.7 nmi), and 2.3×10^3 μm/sec (8.9×10^{-2} in./sec) at 10 km (5.4 nmi). The smallest of these values is approximately 4 times the velocity produced by the maximum expected sonic boom over-pressure.

The ratio of energies for a 3.2 M_L earthquake to a 2.0 M_L event is 15. Velocity is related to energy as the square root of the energy or in this case, a ratio of 4. Thus, a 2.0 M_L earthquake occurring within 10 km (5.4 nmi) of an archeological site can be expected to generate ground motions comparable to those caused by sonic booms. Events of this magnitude, or larger, have been reported in the Valentine MOA, though the frequency of occurrence of an event of this magnitude is uncertain.

5.4 Railroad Valley Sonic Boom Tests

On 19 June 1981, AFGL/LWH and TAC conducted a test in Railroad Valley, Nevada similar to that conducted in the Valentine MOA. In this test five sonic booms were produced by an F-111 flying at Mach 1.1 and altitudes of 3050 and 4000 m AGL (10,000 and 13,000 ft). Sonic booms having over-pressures of 40.2 to 178.5 Pa (0.8 to 3.7 psf) were recorded at ground level by seismic and acoustic arrays located on the alluvial floor of the valley (Francis Crowley, personal communication).

Acoustic admittances calculated for Railroad Valley are representative of the admittances for soil in alluvial basins. Rock materials, as at the archeological sites, can be expected to have lower admittance values. Thus, the admittances found for Railroad Valley can be considered upper limiting values for the areas of interest in the Valentine MOA.

Admittances, calculated in the same manner as used in Section 3.3, were found to range from 1.25 to 4.78 (μm/sec)/Pa [2.4×10^{-3} to 9.0×10^{-3} (in./sec)/ psf] for Railroad Valley. The variation appears to be azimuth dependent and suggests a high variability in the shallow structure near the recording array. These values are from 0.98 to 5.3 times the admittances calculated at the Valentine sites.

Using the maximum admittance found in Railroad Valley and 248.1 Pa (5.19 psf), the maximum over-pressure from carpet booms in the Valentine MOA, an upper limit velocity can be found for the archeological sites. This value is 1.2×10^3 μm/sec (4.7×10^{-2} in./sec) or approximately 4 times the level

---

10. Turnbull, L., Sun, D., Battis, J., and Ringdal, F. (1975) Source Studies in the Near- and Far-Field, Semi-Annual Technical Report No. ALEX(02)-TR-75-02-PART A, Texas Instruments Inc. Dallas, Tex.

predicted on the basis of actual measurements. As in Section 4, using this value as the amplitude in the three directions of motion, the vector sum velocity is found to be 2.1×10^3 μm/sec (8.1×10^{-2} in./sec). This value is still only 8 percent of the strict blasting code limit. The vertical velocity is approximately 1/2 of the velocity generated by the 3.2 M_L earthquake in Bear Valley at an epicenter distance of 10 km (5.4 nmi).

6. THEORETICAL EVALUATION

6.1 The N-Wave

Aircraft traveling at supersonic speeds will produce acoustic shock waves as the result of rapid compression of air along the leading surfaces of the aircraft. Near the aircraft, the pressure wave time history is complicated by the numerous surfaces of the aircraft on which a shock wave can form. The shock front propagates away from the aircraft at the speed of sound in air and, in the far field, can be treated as an acoustic wave having a characteristic wave form known as an N-wave. The N-wave, shown in Figure 4, is defined by a period t_o, a rise time t_r, and a maximum over-pressure given by ΔP. The pressure-time history of an N-wave is given by:

$$p(t) = \begin{cases} \Delta P\left(\dfrac{t}{t_r}\right) & 0 \le t \le t_r \\[2mm] \Delta P[(t_o - 2t)/(t_o - 2t_r)] & t_r \le t \le t_o - t_r \\[2mm] \Delta P[(t - t_o)/t_r] & t_o - t_r \le t \le t_o \quad . \end{cases} \tag{2}$$

Each of the parameters, t_o, t_r, and ΔP, are defined by aircraft design characteristics and velocity while ΔP is also a function of distance from the aircraft to the observer. For a gas, the particle velocity is given by

$$\dot{u}(t) = p(t)/\rho c \quad , \tag{3}$$

where ρ is the gas density and c is the speed of sound in the gas. The maximum particle velocity occurs at $t = t_r$ or $t = t_o - t_r$ when $|p(t)| = \Delta P$. At these times all of the wave energy is kinetic energy and the total energy can be calculated as

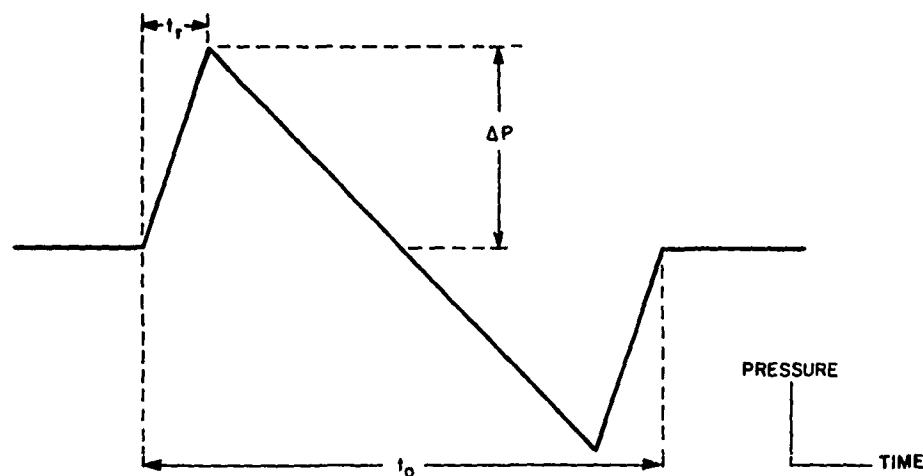$$E_T = KE\Big|_{t=t_r} = 0.5\rho\,[\dot{u}(t_r)]^2 = \Delta P^2/(2\rho c^2) \quad . \tag{4}$$

18

Figure 4. The N-wave and its Defining Characteristics

The shock wave forms a conical wavefront of angle 2ϵ about the aircraft (Figure 5) where

$$\epsilon = \sin^{-1}(c/v) = \sin^{-1}(1/M) \quad , \tag{5}$$

where v is the aircraft velocity and M is the Mach number. In an idealized case with the aircraft in level flight over a flat ground surface, the shock wave will intersect the ground with angle ϵ. In the real atmosphere, where the speed of sound generally decreases with increasing altitude, the intersection angle will steepen. In general this change is sufficiently small to be neglected.

Under most conditions, the ground surface can be assumed to respond to the acoustic wave in air as a rigid body. The incident pressure wave can be considered to be totally reflected off the ground with no energy transmitted into the earth and no deformation of the surface. This is a consequence of the large density contrast between the air and ground. In fact, however, the air and ground are not completely decoupled and acoustic waves impinging on the ground will produce measurable effects in the solid earth. These effects can be classified as (1) a non-propagating elastic response, (2) propagating body waves, and (3) propagating surface waves.

In the following sections each of these phenomena will be considered separately. The magnitude of the ground motions generated by each mechanism will be estimated theoretically for three typical surface geologies found in alluvial basins: alluvial fan and bajada deposits, playa clays, and weathered rock. The seismic properties assumed for these materials are given in Table 1. These properties cover the spectrum of material from very soft soil to rock.

19

Table 1. Seismic Wave Velocities for Typical Alluvial Basin Surficial Materials

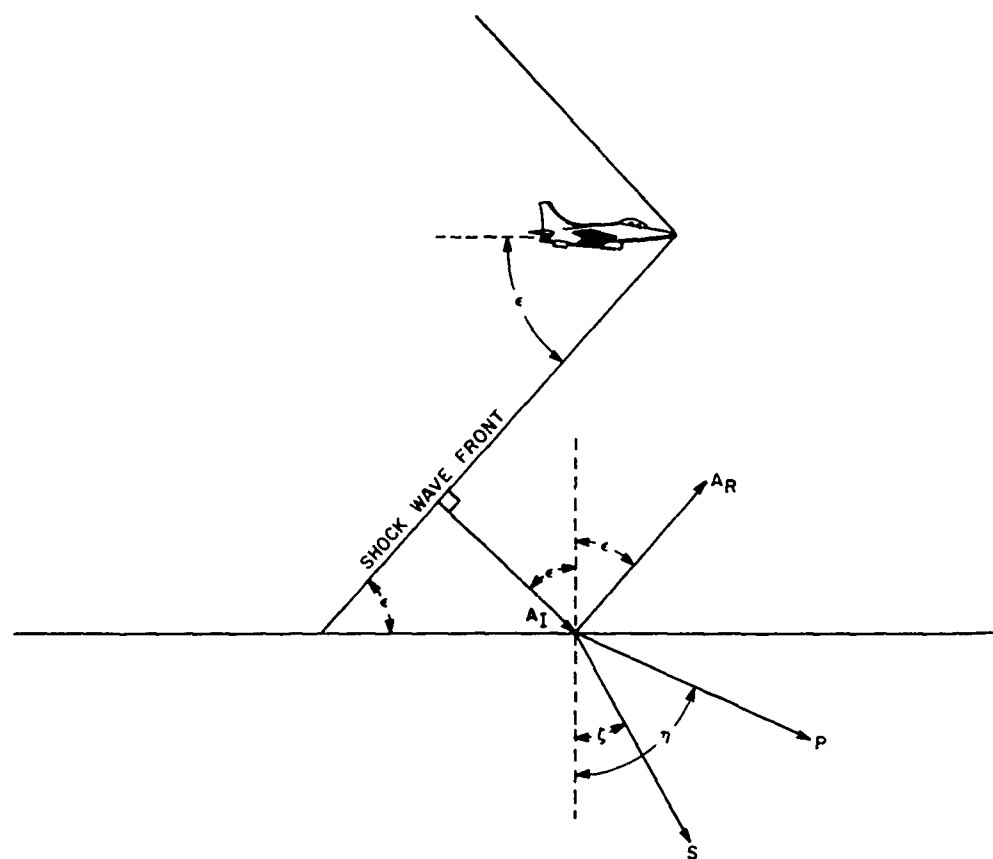| Geologic Medium	Alluvial Basin Setting	α		β		ρ	
		(m/sec)	(ft/sec)	(m/sec)	(ft/sec)	(cm/cm^3)	(lb/ft^3)
Dry Sand and Gravels	Alluvial Fans Bajada Deposits	450	1476	216	709	1.76	109.9
Dry Clays	Playas	750	2460	433	1420	1.76	109.9
Weathered Rock	Mountains Outcrops	2000	6561	1225	4019	2.48	154.8

20

Figure 5. Geometry of the Sonic Shock Wave-Ground Interaction

6.2 Loading Deformations

The passage of a sonic boom over the ground surface is equivalent to a moving, distributed load traveling at a velocity δ given by $\delta = cM$, along the ground surface. This loading produces a non-propagating elastic deformation in the earth. The deformation is a function of the material properties of the ground and the load distribution in time and space. For observations made near the surface, the vertical displacements, $u_g(t)$, at some depth z, can be approximated by:

$$u_g(t) = (z^2/4\pi\mu) \iint_S \{p(x, y, t)/r^3\} dx\, dy$$

$$+ [(\lambda + 2\mu)/(4\pi\mu)(\lambda + \mu)] \iint_S \{p(x, y, t)/r\} dx\, dy \qquad (6)$$

where

$$r = (x^2 + y^2 + z^2)^{1/2} \quad ,$$

λ, μ = Lame's constants for the ground material

and

$p(x, y, t)$ = the loading function.

For a sonic boom, $p(x, y, t)$ can be derived from Eq. (2) where the horizontal spatial coordinates, x and y, are taken relative to the observation point. This equation is strictly valid only for a half-space.

Two assumptions are made to facilitate numerical evaluation of the integrals. First, the wavefront near the point of interest is assumed to be straight in which case $p(x, y, t)$ is only a function of x and t when the x-axis is parallel to the aircraft line of flight. Second, it is assumed that the equation can be discretized and the integrals converted to sums to give:

$$u_g(t) = (z^2/4\pi\mu) \sum_x \sum_y p(x, t)A/r^3 + [(\lambda + 2\mu)/(4\pi\mu)(\lambda + \mu)]$$

$$\sum_x \sum_y p(x, t)A/r \quad , \qquad (7)$$

where A is the area over which $p(x, t)$ is discretized. A singularity occurs in Eq. (7) when $x = y = z = 0$. If the observation point is at depth, however, this problem is avoided. The ground particle velocity $\dot{u}_g(t)$ can be derived by numerical differentiation with respect to time of $u_g(t)$. This formulation has been shown

22

to adequately model the non-propagating elastic deformation associated with sonic booms.[3]

The relationships between peak ground velocity and the various parameters defining pressure loading, t_o, t_r, ΔP, and aircraft Mach number, are sufficiently complex to require full evaluation of Eq. (7) to accurately estimate $\dot{u}_g(t)$ for any specific N-wave. However, several general relationships can be determined. First, fixing all time related parameters, t_o, t_r, and M, peak ground velocity is directly proportional to ΔP. Second, the longer the rise time t_r, the lower is the peak ground velocity. Third, the longer the N-wave period t_o, the higher the ground velocity predicted. Finally, increasing the Mach number M increases the predicted peak velocity. Basically, the last three relationships can be stated as the farther apart in time, and thus space, of the peak over-pressures in the N-wave, the higher the peak particle velocity in the ground.

The first of these relationships makes the evaluation of an admittance, as defined in Eq. (1), possible for the non-propagating surface deformation given a ground structure, a fixed set of N-wave time parameters t_o and t_r, and the aircraft Mach number. For any period t_o, the maximum admittance occurs when the rise time t_r is equal to zero. In Figure 6, admittances are plotted for the three geologic media given in Table 1 for periods t_o, of 0.075 sec and 0.3 sec over the range of Mach numbers from 1.1 to 2.0. The selection of the two values of t_o bound the range of N-wave periods ⁻⁻ most operational aircraft. The range of Mach numbers extends well beyond Mach 1.4, the maximum value expected during training operations in the Valentine MOA.[2] To avoid the singularity at z = 0, all ground motions were derived at a depth of 1 m (3.3 ft).

Over these ranges, the maximum admittance for the non-propagating deformation caused by a sonic boom is created by a 0.3-sec period N-wave at Mach 2.0 occurring in bajada deposits. The admittance is found to be 5.42 (μm/sec)/Pa [0.01(in./sec)/psf]. Using a maximum expected peak over-pressure of 248.1 Pa (5.2 psf) this converts to a peak vector sum ground velocity of 2.3×10^3 μm/sec (0.09 in./sec). This value is less than one-tenth of the blasting code limit. As the deformation is non-propagating, motions of this magnitude can occur only in the bajada deposits. The archeological sites are all situated in rock structures and more realistic estimates of the impact on these sites are obtained by considering admittances for rock. The maximum admittance over these ranges for rock is found to be 0.14 (μm/sec)/Pa [2.7×10^{-4} (in./sec)/psf]. This value gives a peak vector sum velocity of 61.3 μm/sec (2.4×10^{-3} in./sec) or less than 0.25 percent of the blasting code limit.
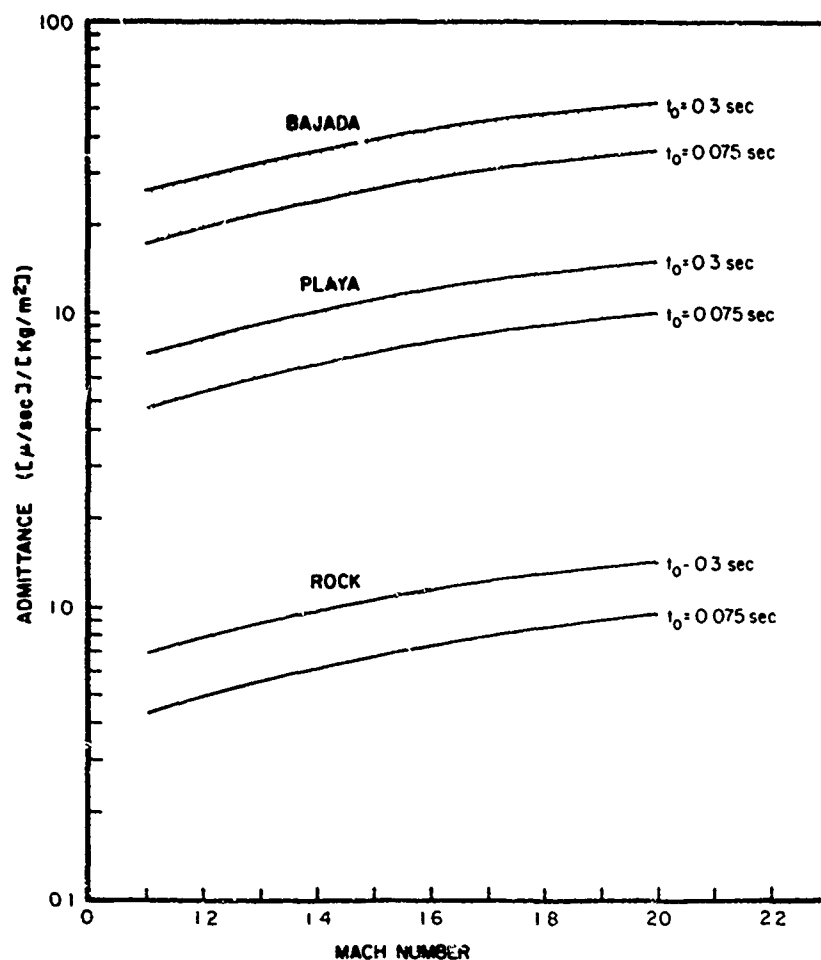
Figure 5. Body Wave Admittances as a Function of Aircraft Velocity,
N-wave Rise Time, and Geologic Structure

6.3 Body Waves

In general an acoustic wave in air A_I, incident on a solid boundary, will give rise to a reflected acoustic wave A_R at the angle ϵ, a transmitted compressional wave P at the angle η, and a transmitted shear wave S at the angle ζ, as shown in Figure 5. By Snell's law the angles of the rays for each wave are given by:

$$\frac{c}{\sin \epsilon} = \frac{\alpha}{\sin \eta} = \frac{\beta}{\sin \zeta} = \delta \tag{8}$$

24

where δ is a constant equal to the apparent velocity of the wave front along the interface and

α = P-wave velocity in the solid

β = S-wave velocity in the solid.

Using a liquid half-space over a solid half-space to model the air-ground interface, theoretical plane wave energy transmission coefficients for this case are given by[11]

$$E_p = [2\rho A\delta^2(\delta^2/\beta^2 - 2)/D]^2 [\rho_s \cot \eta / \rho \cot \epsilon]$$

$$E_s = [-4\rho AG\delta^2/D]^2 [\rho_s \cot \zeta / \rho \cot \epsilon]$$

$$E_r = [(D - 2\rho G\delta^4/\beta)/D]^2 \quad . \tag{9}$$

where

$$D = [\rho G\delta^4/\beta^2] + \rho_s \beta^2 A[(\delta^2 - 2)^2 + 4GH]$$

ρ_s = density of the solid

and

$$A = (\delta^2/\alpha^2 - 1)$$

$$G = \begin{cases} (\delta^2/\alpha^2 - 1)^{1/2} & \delta > \alpha \\ -i(1 - \delta^2/\alpha^2)^{1/2} & \delta < \alpha \end{cases} \qquad H = \begin{cases} (\delta^2/\beta^2 - 1)^{1/2} & \delta > \beta \\ -i(1 - \delta^2/\beta^2)^{1/2} & \delta < \beta \end{cases}$$

with all other parameters as previously defined. The values of E_p and E_s are the ratios of energy of the transmitted P and S wave, respectively, to the incident wave energy and E_r gives the energy ratio of the reflected acoustic wave.

Using these equations the transmitted energy ratios were calculated for three different surficial velocity structures common to alluvial basins of the southwestern United States. In all calculations the air density and speed of sound were

11. Ewing, W., Jardetzky, W., and Press, F. (1957) Elastic Waves in Layered Media, McGraw-Hill Book Co., Inc., New York.

25

taken to be those of the U.S. Standard Atmosphere of 1976 at 1000 m (3281 ft) elevation, 1.11 kg/m^3 (0.0022 slugs/ft^3) and 336.43 m/sec (1103.8 ft/sec), respectively. [12] The calculated coefficients, as functions of angle of incidence of the wave front are shown in Figures 7 through 9. In addition, Mach numbers for an aircraft in level flight required to produce given angles of incidence are shown.

In Figure 7, velocities typical of dry sands and gravels found in alluvial fans and bajada deposits were used in the calculations. In this case, the speed of sound in air is greater than the shear wave velocity and energy is transmitted at all angles of incidence. From Mach 1 to 1.34, only S-waves are generated and at higher speeds P- and S-waves will result. Above Mach 1.06 total energy transmission is less than 1 percent of the incident wave energy, where the total energy transmitted is given by the sum of E_p and E_s. (Except during the subsonic to supersonic transition, aircraft would typically avoid speeds between Mach 0.9 and
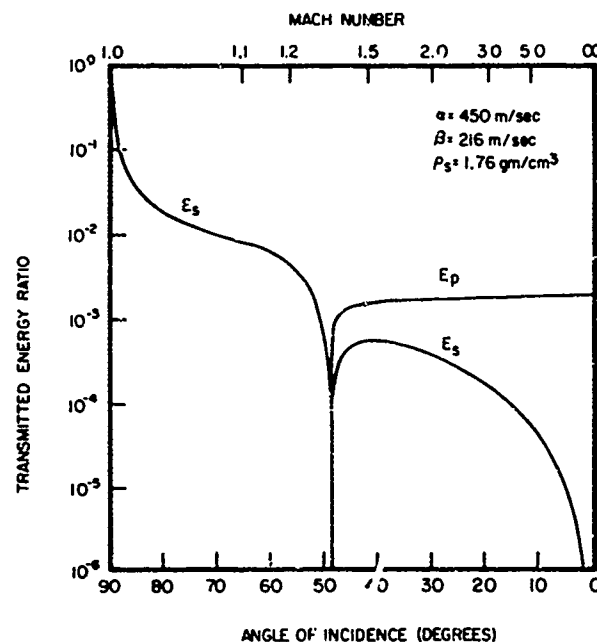

Figure 7. Body Wave Energy Transmission Ratios as Functions of N-wave Angle of Incidence for Alluvial Fan and Bajada Deposits

12. Kantor, A.J., Minzner, R.A., and Quiroz, R.S., Eds. (1976) U.S. Standard Atmosphere, 1976, U.S. Government Printing Office, Washington, D.C.
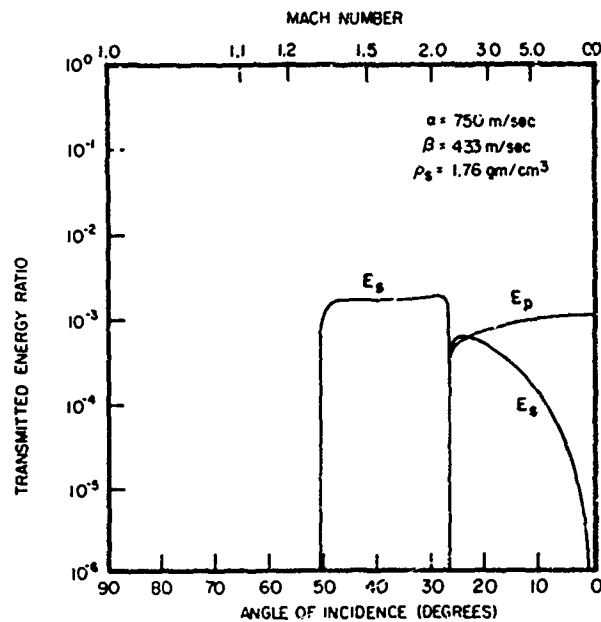
Figure 8. Body Wave Energy Transmission Ratios as Functions of N-wave Angle of Incidence for Playa Clays
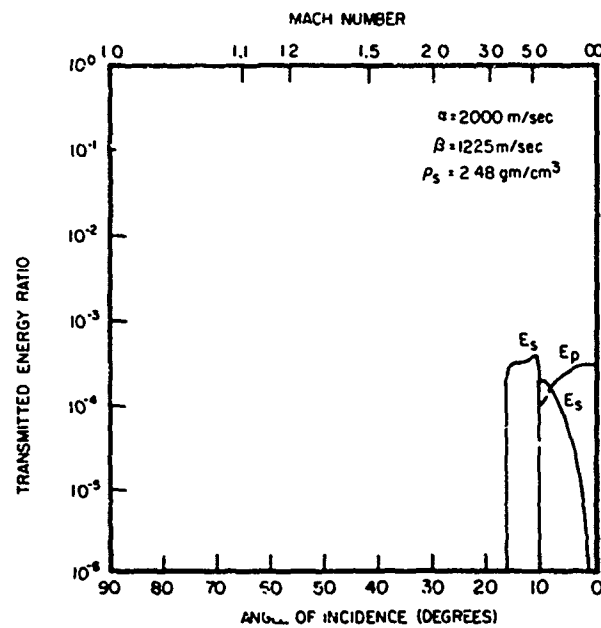

Figure 9. Body Wave Energy Transmission Ratios as Functions of N-wave Angle of Incidence for Weathered Rocks

27

1.1 due to unstable aerodynamic conditions.) Transmission coefficients for playa clays are shown in Figure 8. All energy is reflected from the surface below Mach 1.29 and maximum energy transmission occurs at Mach 2.15 with 0.158 percent energy transmission. In Figure 9, velocities typical of weathered rock were used. Total energy reflection occurs below Mach 3.64 and maximum energy transmission is 0.039 percent at Mach 5.76. It should be noted that roughness in the ground surface will modify the apparent angle of incidence at any point; thus, energy may be transmitted into the ground at lower equivalent Mach numbers than stated.

These values, however, provide a means of evaluating the maximum particle velocities of the transmitted seismic waves generated by a sonic boom. The total energy of the incident acoustic wave, given by Eq. (4), multiplied by the appropriate energy transmission coefficient, gives the maximum kinetic energy in either the P or S-wave. Solving for particle velocity in the solid from the maximum transmitted energy gives

$$\dot{u}_{g(max)} = (E/\rho_s \rho c^2)^{1/2} \Delta P \quad , \tag{10}$$

where $\dot{u}_{g(max)}$ is the maximum ground particle velocity and E is either E_p or E_s. Considering only transmitted body waves, the quantity $(E/\rho_s \rho c^2)^{1/2}$ is the body wave admittance $Y(f)$ as defined in Eq. (1). For the three velocity structures discussed above, the maximum body wave admittances for all angles of incidence are found to be 6.85 $(\mu m/sec)/Pa$ [1.3×10^{-2} (in./sec)/psf] for bajada deposits, 0.27 $(\mu m/sec)/Pa$ [5.1×10^{-4} (in./sec)/psf] for playa clays, and 0.11 $(\mu m/sec)/Pa$ [2.1×10^{-4} (in./sec)/psf] for weathered rock.

It would be expected that in the field, lower values would be measured, as the average angle of incidence of the incoming wave would differ from the angle giving the maximum value of E. In bajada deposits the measured body wave admittance would be expected to be much lower than the maximum value, as the maximum of E is more than 100 times larger than the average value over all angles.

6.4 Surface Waves

In addition to the non-propagating deformation and the transmitted body waves, a sonic boom incident on the ground will also generate Rayleigh waves, which propagate along the ground surface. Generally the energy transferred from the acoustic wave into the Rayleigh mode is small. However, under certain restricted conditions, resonant coupling between the air wave and the Rayleigh wave can occur at discrete frequencies. These phenomena result in significant amplification of Rayleigh wave ground motions at these frequencies. A complete mathematical

28

treatment of these phenomena is beyond the scope of this report. However, a simple model demonstrating the generation of air-coupled Rayleigh waves and the conditions of their occurrence is presented in this section.

A simplified model of air-coupled Rayleigh wave generation can be developed by considering a moving, impulsive load on the surface of a constant velocity half-space. Consider the load to be discretized as a series of impulsive loads applied to the surface at spacings of Δx with time separations of Δt. The velocity of the load V_L, is given by $\Delta x / \Delta t$. A load is applied at time $t = o$ and $x = o$. This load will generate a Rayleigh wave pulse along the air-ground interface with a velocity C_R, known as the phase velocity. At the time of the next load application, Δt, the Rayleigh wave has traveled a distance given by $C_R \Delta t$ while the load has moved Δx or $V_L \Delta t$ (Figure 10). Assuming constant load amplitude, this load will also generate a Rayleigh pulse of equal amplitude to the first pulse. If C_R does not equal V_L, the two pulses will propagate as discrete pulses. However, if C_R is equal to V_L then the second pulse will be superimposed on the first Rayleigh pulse. Neglecting attenuation, the amplitude of Rayleigh wave will double. Each subsequent load application will increase the amplitude arithmetically. These phenomena are the resonant coupling of the air-coupled Rayleigh wave. For a sonic boom, V_L is the apparent velocity of the sonic boom along the ground surface given by δ in Eq. (8).

While demonstrating the mechanism of resonant coupling, this simple model cannot show the full complexity of air-coupled Rayleigh wave generation by sonic booms. A realistic model of near-surface geology at most sites would typically require one or more layers of different seismic velocities over the constant velocity half-space. When seismic velocities vary with depth, as in this case, the phase velocity is not constant but a function of frequency of the wave. In addition, the sonic boom is not a single pressure load but a distributed load on the ground. Both of the properties of the problem affect the development of the air-coupled phase.

For the Rayleigh wave, propagation is restricted to the plane of the ground surface, however, the wave produces particle motions away from the surface. The amplitude of these motions decay away from the surface at a rate proportional to the wavelength or period of the signal. The phase velocity C_R at any particular period can be viewed as some function of the weighted averages of the S-wave velocities over depth where the weighting function is related to the amplitude decay rate. Thus, at very high frequencies all significant motion is restricted to very shallow depths and the phase velocity will approach that of a half-space having the seismic velocities of the first layer of the model. At very low frequencies the particle motion extends deep into the model half-space and the weighted average velocities approach those of the half-space. These two conditions
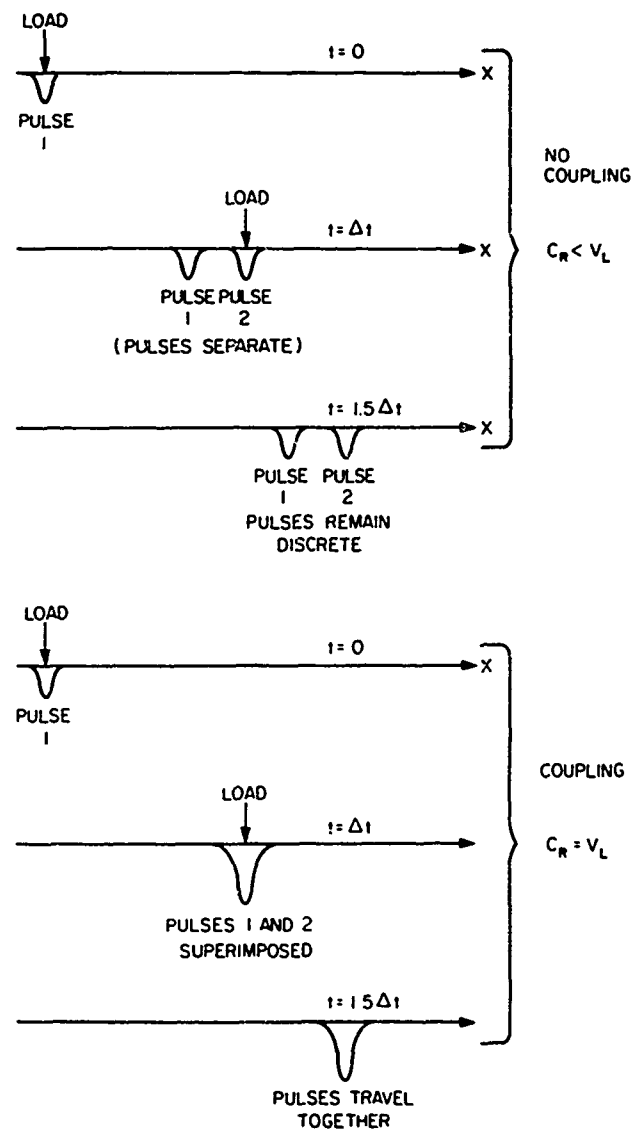
29

Figure 10. Simplified Model of Air-Coupled Rayleigh
Wave Generation

provide limits on the phase velocity function for the layered model. As seismic velocities tend to increase with depth the phase velocity will tend to increase with period.

The half-space phase velocities can be evaluated by solving for the real root of the Rayleigh equation given by:

$$C_R^6 - 8C_R^4\beta^2 + C_R^2\beta^4(24 - \beta^2/\alpha^2) - 16\beta^6(1 - \beta^2/\alpha^2) = 0 \quad , \tag{11}$$

where $0 < C_R < \beta < \alpha$.[13] For most geologic media a first order estimate of phase velocity is given by $C_R \sim 0.9\beta$. Solving this equation using the seismic velocities given in Table 1 gives half-space phase velocities for bajada deposits, playa clays, and weathered rocks of 202, 398, and 1116 m/sec (663, 1306, and 3661 ft/sec), respectively.

The first condition for the generation of air-coupled Rayleigh waves from a sonic boom is that the apparent velocity along the ground surface of the sonic boom, δ, must be greater than the high frequency phase velocity limit, $C(f_\infty)$, and less than the low frequency limit, $C_R(f_o)$ or:

$$C_R(f_\infty) < \delta < C_R(f_o) \quad .$$

The upper bound, $C_R(f_o)$ is of little interest as it is typically much higher than the operational speeds of aircraft. The lower bound, $C_R(f_\infty)$, corresponds to the phase velocity of the surface layer taken as a half-space as calculated in the preceding paragraph. To have any potential for generating an air-coupled wave in weathered rock, an aircraft would have to exceed Mach 3.3. For playa clays the lower limit corresponds to an airspeed of Mach 1.18 while for bajada deposits any aircraft exceeding the speed of sound could produce an air-coupled Rayleigh wave as $C_R(f_\infty)$ is less than the speed of sound in air.

A match between the apparent velocity of the sonic boom, δ, and the phase velocity of a given frequency of the Rayleigh wave is not sufficient to ensure the generation of the air-coupled surface wave. The N-wave must also have energy at the same frequency. The amplitude spectra for the idealized N-wave with $t_r = 0$ and $t_o = 0.075$ and 0.3 sec are plotted in Figure 11. It is apparent from this figure that the energy distribution with frequency is highly dependent on the N-wave duration and, over significant portions of the spectrum the energy in the N-wave will be very small. Thus, even if an air-coupled wave is generated,

13. Bullen, K. (1963) An Introduction to the Theory of Seismology, Cambridge University Press, New York.
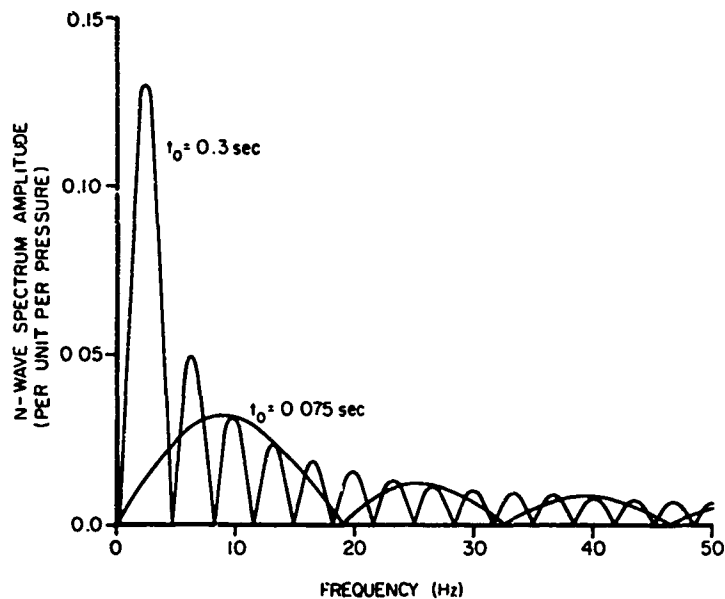
31

Figure 11. Theoretical Amplitude Spectra for N-waves
with $t_r = 0$ and $t_o = 0.075$ and 0.3 sec

insufficient energy may exist at that frequency to produce a significant amplitude surface wave.

The evaluation of the frequency-phase velocity relationship for a given velocity structure is a well known procedure.[11] However, the relationship is highly dependent on the specific geology of the site of interest. The energy content of the N-wave is also variable with the speed of the aircraft, design factors and other effects. Thus, the evaluation of the amplitude of air-coupled surface waves must be conducted on a case by case basis. However, using a worst case scenario of a 0.075-sec duration sonic boom, a peak over-pressure of 235.4 Pa (5 psf) and a velocity structure tuned to maximize the air-coupled phase, a maximum amplitude of approximately 10 percent of the strict blasting code limit was attained. (Francis Crowley, personal communication, 1980). In addition, the analysis provided above assumes a level surface and a laterally constant seismic velocity structure. If the topography or velocity structure is highly irregular in the lateral directions, then the air coupling cannot be sustained over a long enough distance to produce significant ground motion. Even if generated, when the air-coupled wave impinges on a region of significant seismic velocity gradient, such as at an alluvial basin edge, a high degree of scattering can be expected and the amplitude of the air-coupled phase will be greatly attenuated.

32

7. CONCLUSIONS

Seismo-acoustic recordings of sonic booms were made at two sites in the Valentine MOA. Each location was selected as representative of a class of significant archeological sites found within the MOA. These studies indicate that sonic booms are unlikely to cause damage to the archeological finds. The expected motions are, at worst, 8 percent of the limits set by strict blasting codes and comparable to velocities that could be produced by local earthquakes which have occurred in the Valentine area.

At these levels of motion, competent rock will be unaffected by the transmission of seismic waves. The predicted velocity levels are unlikely to initiate either fracture or spalling in rocks. However, it is possible that in rocks where natural meteorological action has initiated these erosive mechanisms the sonic boom induced motion could accelerate the processes to some small degree. In other words, a sonic boom might trigger the final separation of one rock surface from another. For this to happen, the natural processes of erosion, working over a long period of time, would be required to develop a highly unstable condition in which the sonic boom provides the last, destabilizing force. Without the sonic boom, however, the natural forces would, in a relatively short time, have produced the same end effect.

To illustrate this point a simplified model of a spalled rock can be constructed. In this model the defoliated lamina is considered to be a thin slab of rock having a surface area, A, in contact with an infinite rock mass. Only some fraction of the contact surface area, νA, remains bonded to the rock mass. Then, for the slab to remain attached under its own weight, the static force equilibrium requires that

$$W \mu \cos \theta + \nu A \tau_0 - W \sin \theta = 0 \quad , \tag{12}$$

where W is the weight of the spalling slab, μ is the coefficient of static friction, τ_0 is the cohesion intercept of the Mohr-Coulomb failure criterion, and θ is the angle of the contact surface to the horizontal. It can easily be shown that ν is maximized when θ equals 90°; that is, the contact surface is vertical. Then, if the slab is assumed to be of uniform thickness t, the weight W can be written as

$$W = \gamma At \quad ,$$

where γ is the unit weight of the rock. Substituting this relation into Eq. (12) and solving for ν yields the equation

$$v_s = \gamma t / \tau_o \quad , \tag{13}$$

where v_s is the minimum fraction of bonded surface area to hold the slab against only its own weight. Under this condition any additional downward force will cause complete separation of the lamina. For the dynamic case, when the rock mass undergoes a rigid body acceleration a, parallel to the contact surface, Eq. (13) will take the form:

$$v_d = \gamma t \left(1 + \frac{a}{g}\right) / \tau_o \tag{14}$$

where v_d is the minimum v value required for stability of the lamina in the dynamic case.

Very conservative estimates for v_s and v_d can be obtained using a unit weight of 3000 kg/m^3 (187.3 pcf), a cohesion intercept of 3.9×10^5 Pa (8.2×10^3 psf) and a thickness of 0.05 m (2.0 in.). To indicate the inherent conservatism of these values, a typical sedimentary rock has a cohesion intercept 25 to 50 times greater than that used in this calculation.[4] For the dynamic case, the acceleration a can be estimated from a peak velocity using the relationship:

$$a_{max} = 2\pi f V_{max}$$

where f is the frequency of the peak velocity. Using the maximum particle velocity estimated in this report for any form of ground motion and a conservative frequency of 50 Hz, the maximum acceleration is found to be 0.79 m/sec^2 (2.6 ft/sec^2). Then, v_s is found to be 0.37 percent and v_d is found to be 0.40 percent. In other words, if the defoliated slab remains attached to the rock mass at less than 1 percent of its total surface area it will withstand the worst expected effects of sonic booms, and the value required for dynamic stability is insignificantly larger than that required for static equilibrium.

References

1. Haskell, N. (1951) A note on air-coupled surface waves, Bull. Seism. Soc. Amer. 41:295-300.

2. (1979) Draft Environmental Impact Statement, Supersonic Flight Operations in the Valentine Military Operations Area, Dept. of the Air Force, Holloman AFB, New Mexico.

3. Goforth, T., and McDonald, J. (1968) Seismic Effects of Sonic Booms, NASA Report No. CR-1137, Teledyne Geotech, Garland, Tex.

4. Handin, J. (1966) Strength and Ductility, in Handbook of Physical Constants, S. Clark, Jr., Ed., The Geol. Soc. Amer., New York, N.Y.

5. Jaeger, J.C., and Cook, N.G.W. (1969) Fundamentals of Rock Mechanics, Methuen & Co. Ltd, London.

6. Dade County, Florida Code, Section 13-12.

7. Ortaid, L. (1972) Blasting operations in the urban environment, Assoc. Engin. Geol. 9:27-46.

8. Dumas, D., Dorman, H., and Latham, G. (1980) A reevaluation of the August 16, 1931 Texas earthquake, Bull. Seism. Soc. Amer. 70:1171-1180.

9. McGuire, R. (1974) Seismic Structural Response Risk Analysis Incorporating Peak Response Regressions on Earthquakes Magnitude and Distance, Dept. Civil Eng. Research Report No. R47-51, Mass. Inst. Tech., Cambridge, Mass.

10. Turnbull, L., Sun, D., Battis, J., and Ringdal, F. (1975) Source Studies in the Near- and Far-Field, Semi-Annual Technical Report No. ALEX(02)- TR-75-02-PART A, Texas Instruments Inc., Dallas, Tex.

11. Ewing, W., Jardetzky, W., and Press, F. (1957) Elastic Waves in Layered Media, McGraw-Hill Book Co., Inc., New York.

12. Kantor, A.J., Minzner, R.A., and Quiroz, R.S., Eds. (1976) U.S. Standard Atmosphere, 1976, U.S. Government Printing Office, Washington, D.C.

13. Bullen, K. (1963) An Introduction to the Theory of Seismology, Cambridge University Press, New York.

Abbreviations and Units

AFGL/LWH	– Applied Crustal Physics Branch, Air Force Geophysics Laboratory
AGL	– Above Ground Level
cm	– centimeters (10^{-2} meter, 0.394 inch)
HQ TAC/DEEV	– Environmental Planning Division, Headquarters, Tactical Air Command
km	– kilometers (10^3 meter, 0.540 nautical mile)
ln	– natural logarithm
m	– meters (3.281 feet)
μm	– micrometer (10^{-6} meter, 3.94×10^{-5} inch)
M	– Mach Number
m_b	– body wave magnitude
M_L	– local magnitude
MOA	– Military Operations Area
MSL	– Mean Sea Level
nmi	– nautical miles (1.151 statute miles)
Pa	– pascal (0.0209 psf)
pcf	– pounds per cubic foot
psf	– pounds per square foot
slugs/ft^3	– engineering system unit of mass density (515.4 kg/m^3)